NASA TECHNICAL MEMORANDUM

NASA TM X-73994

NASA TM X-73994

FATIGUE DAMAGE OF NOTCHED BORON/EPOXY LAMINATES UNDER CONSTANT AMPLITUDE LOADING

G. L. Roderick

and

J. D. Whitcomb

Presented at the ASTM Symposium on Fatigue of Filamentary Composites, November 15-18, 1976, Denver, Colorado.

NATIONAL AERONAUTICS AND SPACE ADMINISTRATION
LANGLEY RESEARCH CENTER, HAMPTON, VIRGINIA 23665

1. Report No.	2. Government Accession No.	3. Recipient's Catalog No.
TM X-73994		

4. Title and Subtitle	5. Report Date
FATIGUE DAMAGE OF NOTCHED BORON/EPOXY LAMINATES UNDER CONSTANT AMPLITUDE LOADING	December 20, 1976
	6. Performing Organization Code
7. Author(s)	8. Performing Organization Report No.
G. L. Roderick and J. D. Whitcomb	
	10. Work Unit No.
9. Performing Organization Name and Address	506-17-27-01
United States Army Air Mobility R&D Laboratory NASA-Langley Research Center Hampton, VA 23665	11. Contract or Grant No.
	13. Type of Report and Period Covered
12. Sponsoring Agency Name and Address	Technical Memorandum
National Aeronautics and Space Administration Washington, D.C. 20546	14. Sponsoring Agency Code

15. Supplementary Notes

Paper presented at ASTM Symposium on Fatigue of Filamentary Composites, November 15-18, 1976, Denver, Colorado.

16. Abstract

Fatigue damage in (0,±45) and (0,±45,90) boron/epoxy laminates was studied with X-ray radiography and scanning electron microscopy. In addition, limited tests for residual strength and stiffness were performed.

Initially, fatigue damage in both (0,±45) and (0,±45,90) laminates occurred as intralaminar cracks around the edge of the hole. Then, whenever further damage developed, intralaminar cracks in the ±45-degree plies began to propagate from the edge of the hole. Finally, in both type laminates, primarily ±45-degree fibers broke (prior to two-piece failure) where intralaminar cracks in the ±45-degree plies had occurred. In the (0,±45) laminates, the 45-degree plies developed intralaminar and transthickness cracks along lines parallel to the loading axis and tangent to the hole in the test specimen. This damage, which was most pronounced under compression loads, had little effect on either strength or stiffness. In contrast, in the (0,±45,90) laminates, the ±45-degree plies developed intralaminar cracks transverse to the loading axis. The transverse damage, which occurred primarily under tension loads, affected the residual strength but not the stiffness and frequently resulted in catastrophic failure across the notch.

The results of this study suggest that in boron/epoxy laminates the 45-degree plies play a key role in the fatigue process of boron/epoxy laminates that contain them. The fatigue process in the ±45-degree plies starts as intralaminar matrix cracks.

17. Key Words (Suggested by Author(s)) (STAR category underlined)	18. Distribution Statement
Composite Materials, Boron/Epoxy Laminates, Fatigue (Materials) Damage, Radiography, Microscopy	

19. Security Classif. (of this report)	20. Security Classif. (of this page)	21. No. of Pages	22. Price*
UNCLASSIFIED	UNCLASSIFIED	30	$4.00

*Available from { The National Technical Information Service, Springfield, Virginia 22151
STIF/NASA Scientific and Technical Information Facility, P.O. Box 33, College Park, MD 20740

FATIGUE DAMAGE OF NOTCHED BORON/EPOXY LAMINATES UNDER CONSTANT AMPLITUDE LOADING

by

G. L. Roderick*

and

J. D. Whitcomb**

* US Army Air Mobility Research and Development Laboratory, NASA-Langley Research Center, Hampton, Virginia

**NASA-Langley Research Center, Hampton, Virginia

ABSTRACT

Fatigue damage in (0,±45) and (0,±45,90) boron/epoxy laminates was studied with X-ray radiography and scanning electron microscopy. In addition, limited tests for residual strength and stiffness were performed.

Initially, fatigue damage in both (0,±45) and (0,±45,90) laminates occurred as intralaminar cracks around the edge of the hole. Then, whenever further damage developed, intralaminar cracks in the ±45-degree plies began to propagate from the edge of the hole. Finally, in both type laminates, primarily ±45-degree fibers broke (prior to two-piece failure) where intralaminar cracks in the ±45-degree plies had occurred. In the (0,±45) laminates, the 45-degree plies developed intralaminar and transthickness cracks along lines parallel to the loading axis and tangent to the hole in the test specimen. This damage, which was most pronounced under compression loads, had little effect on either strength or stiffness. In contrast, in the (0,±45,90) laminates, the ±45-degree plies developed intralaminar cracks transverse to the loading axis. This transverse damage, which occurred primarily under tension loads, affected the residual strength but not the stiffness and frequently resulted in catastrophic failure across the notch.

The results of this study suggest that in boron/epoxy laminates the 45-degree plies play a key role in the fatigue process of boron/epoxy laminates that contain them. The fatigue process in the ±45-degree plies starts as intralaminar matrix cracks.

KEY WORDS: Composite materials, boron/epoxy laminates, fatigue (materials) damage, radiography, microscopy.

INTRODUCTION

Composite materials research has, over the past decade, developed into a prime effort in materials research. Because composites have high strength-to-weight ratios and can be tailored to meet specific requirements for strength and stiffness, they are structurally advantageous for civil and military aircraft. Of course, composite materials used in aircraft must be reliable; accordingly, their fatigue behavior should be understood.

Previous investigators noted that the fatigue behavior of a composite is significantly affected by fiber orientation and the stacking sequence. Durchlaub and Freeman (1) noted that notched boron/epoxy laminates subjected to repeated loads failed either parallel or transverse to the loading axis depending on the fiber orientation. Foye and Baker (2) noted that the stacking sequence could affect the fatigue life of composite laminates by an order of magnitude. These effects of fiber orientation and stacking sequence on composite fatigue behavior cannot be understood without considering the fatigue process on the interlaminar and intralaminar level. Unfortunately, the fatigue process on this microlevel has yet to be clearly defined.

Williams and Reifsnider (3) have studied the fracture surfaces of fatigue-fractured boron/epoxy and boron/aluminum laminates with a scanning electron microscope and have identified debonding, fiber breakage, delamination, and matrix cracking as mechanisms of the fatigue process. Other researchers have noted similar mechanisms in other material systems. But for the most part, neither the primary mechanisms that initiate the fatigue process nor the sequence in which the mechanisms occur have been

clearly identified. A first step in understanding the fatigue process in a wide range of composites is to identify the fatigue process in a specific composite.

Accordingly, the objective of this paper is to identify the primary fatigue mechanisms and the sequence of events in fatigue of notched boron/epoxy laminates. The objective was approached in several steps. First, the fatigue processes in various laminates were determined by examining fatigued specimens with X-ray radiography and scanning electron microscopy. Then, the fatigue processes for the laminates were compared and the primary mechanisms and sequence of events were identified. Next, the macroscopic behaviors of the various laminates with differing fiber orientations and stacking sequences were characterized by testing for stiffness and residual strength. Finally, the fatigue processes and macroscopic behavior were correlated.

SYMBOLS LIST

E^*	Effective modulus computed from applied stress and deflection measured over a 10 cm gage length, MPa
L	Gage length, cm
R	Ratio of minimum to maximum stress in fatigue cycle
w	Width of the specimen, m
α	Fiber orientation angle, deg
σ	Stress, MPa
δ	Deflection, m

EXPERIMENTAL PROCEDURE AND APPARATUS

Specimens and Loading

The specimen configuration is shown in Figure 1. Drilled holes in the specimens represented discontinuities that may exist in an actual structure. They also localized fatigue damage for convenient observation. A few unnotched specimens were tested for baseline data. Two types of laminates were considered: one had fibers oriented at 0° and ±45°; the other had fibers oriented at 0°, ±45°, and 90°. Two stacking sequences for each type laminate were studied: $(0/\pm45/0)_s$, $(+45/0/-45/0)_s$, $(90/\pm45/0)_s$, and $(45/90/-45/0)_s$. The specimens, which contained 55% fibers by volume, were made from 0.1 mm (.004 in.) boron fibers and AVCO 5505 epoxy resin. They were cured at 449° K for ninety minutes.

The specimens were fatigue tested under constant amplitude, load controlled, sinusoidal axial loading with R = .05 or R = 20. All of the fatigue tests were conducted on servohydraulic test machines at a frequency of 10 Hz, whereas some of the static tests were conducted on static tensile test machines. Guide plates prevented buckling during the compression tests. The maximum absolute gross section stress applied during cyclic loading was 318 MPa for the (0,±45) laminates and 191 MPa for the (0,±45,90) laminates. These stresses, which were approximately two thirds of the static ultimate tensile strength of the notched specimens, produced nominal axial strains initially of .0027 and .0024 for the (0,±45) and (0,±45,90) laminates respectively. All measurements were taken in U.S. Customary Units.

Monitoring Fatigue Damage

Fiber breakage, matrix cracking, and axial stiffness were monitored and residual strength was determined. Fiber breakage was detected by taking radiographs periodically during fatigue tests (specimens were X-rayed at zero load). Soft X-rays were sent through a beryllium window by a point source operating at 50 kilovolts and 20 milliamperes. The point source was 30 cm from the specimen. High resolution photographic glass plates were processed and then examined on a metallograph at a magnification of about 50 times. At this magnification, the breaks in the tungsten core of the boron fibers could be easily seen. The breaks in the tungsten cores were assumed to coincide with fiber breaks. Figure 2 shows a typical radiograph and magnified breaks.

The matrix damage in unfailed fatigued specimens, was detected by examining a series of cross-sections, about six per specimen, in a scanning electron microscope. Typically, for each laminate different specimens were examined after 10^7, 5×10^6, and 1×10^6 load cycles. Prior to sectioning each specimen was X-rayed.

The variations of stiffness were obtained by periodically recording the peak elongation over a 10 cm gage length for both notched and unnotched specimens throughout the tension fatigue tests. The deflection was measured with two linear variable differential transformers (LVDT), arranged as shown in Figure 3. The LVDTs recorded deflections within .003 mm. Residual tensile strengths were measured after 10 million tensile load cycles.

The number of tests performed on each laminate is shown in the following table:

Laminate	Tension Fatigue	Compression Fatigue	Virgin Tension Static
$(0/\pm45/0)_s$	7	4	5
$(45/0/-45/0)_s$	5	3	4
$(90/\pm45/0)_s$	10	3	8
$(45/90/-45/0)_s$	9	3	3

For the fatigue tests radiographs were taken of every specimen, micrographs were taken of three specimens for each laminate, stiffness was monitored for all tension fatigue tests, and residual strengths were determined for at least two tension specimens of each laminate.

RESULTS AND DISCUSSIONS

Microscopic fiber and matrix damage is discussed first. Then macroscopic fatigue behavior is discussed in terms of stiffness and residual strength. Finally, the fatigue behavior of both type laminates are compared.

(0,±45) Laminates

Fiber Damage

Fiber damage in the $(0,\pm45)$ laminates was similar for both stacking sequences under either tension or compression loads, but more fibers broke under compression loads. As a typical example, Figure 4 shows where fibers broke in the first quadrant of a $(45/0/-45/0)_s$ laminate after various numbers of tension load cycles. On Figure 4 (noting that the fiber orientation angle, α, was measured clockwise from the loading axis) the open symbols show where -45-degree fibers broke while the solid symbols

show where the 0-degree fibers broke. On the figure the different shaped symbols indicate the number of cycles at which the fiber breaks were detected (the specimen was X-rayed before loading and thereafter only at the intervals indicated by the different symbols).

Figure 4 shows that, in the first quadrant, primarily -45-degree fibers broke in a narrow band, about a millimeter wide, parallel to the loading axis. Typically, each fiber broke only in one place. In general, as load cycles increased, -45-degree fibers broke further away from the hole, and the density of fiber breaks near the hole increased. However, even after 10^7 load cycles only about fifty percent of the -45-degree fibers had broken within a hole diameter of the transverse centerline of the specimen.

In the third quadrant of the specimen, fiber damage was similar to damage in the first quadrant, namely, an equivalent number of fibers broke in the -45-degree plies. In the second and fourth quadrants, breaks in the +45-degree fibers were predominant. Thus, all the broken $\pm$45-degree fibers were those that a plane stress analysis showed had been loaded in maximum tension.

On the basis of all the tests of the $(0,\pm45)$ laminates, several observations about fiber damage can be made. In similar tests, the number of fibers that broke within a hole diameter of the transverse centerline of the specimen varied from a few percent to over fifty percent. Initially, under either tension or compression loads 45-degree fibers that were in maximum tension broke. Although in one test these initial breaks occurred symmetrically with respect to the hole center, in most cases they occurred either in the first and third or second and

fourth quadrants. In one compression test, after most of the 45-degree tension fibers broke (more tension fibers broke in this test than in any other test), the 45-degree compression fibers also broke. This observation suggests that after most of the 45-degree maximum tension fibers break, additional load cycles will cause 45-degree compression fibers to break.

Matrix Damage

Matrix damage was similar for both stacking sequences of the $(0,\pm45)$ laminates. As typical examples, micrographs of a $(0/\pm45/0)_s$ laminate are shown. Figure 5 shows three micrographs of matrix damage in an unfailed $(0/\pm45/0)_s$ laminate after 10^7 tensile load cycles. The micrographs were taken on three cross sections that are indicated on the sketches by section lines.

The micrograph taken at section A-A shows three types of matrix failure. First, near the surface of the laminate, matrix has disbonded from the fibers closest to the surface. This type of damage can be observed with the naked eye and is expected to play a minor role in the fatigue damage process. Consequently, it will not be discussed in what follows. Second, in a plane parallel to the loading axis and perpendicular to the plane of the laminate, transthickness matrix cracks developed. Third, in the plane of the laminate, intralaminar matrix cracks developed in the ±45-degree plies.

The micrograph taken at section B-B shows typical intralaminar cracks in the -45-degree plies near the edge of the hole. The micrograph taken at section C-C shows intralaminar cracks extend from the edge of the hole to transthickness cracks.

The sketch on Figure 5 shows the extent of the two types of cracks. The solid irregular lines show the location of transthickness cracks and the shaded areas show the region of intralaminar cracks in the ±45-degree plies. Both of these cracks run through the matrix in different planes from fiber to fiber. However, typically, the cracks go around the fibers rather than through them.

Figure 6 shows three micrographs of matrix damage in an unfailed $(0/\pm45/0)_s$ laminate after 10^7 compression load cycles. These micrographs show damage similar to, but more severe than, that observed in the specimen tested in tension (Figure 5). The first micrograph taken at section A-A shows intralaminar cracks in the -45-degree plies and transthickness cracks. The micrograph also shows voids where portions of fibers and matrix are missing. Most likely, in these areas a number of transthickness and intralaminar cracks had coalesced and left bits of matrix and fiber unsupported. These bits were probably washed away by the sectioning and cleaning process.

The second micrograph taken at section B-B, near the hole, shows that intralaminar cracks developed in both the 0 and ±45-degree plies. However, micrographs of other specimens tested to 5×10^6 load cycles showed intralaminar cracks only in the ±45-degree plies. Thus, the 0-degree plies probably cracked after the ±45-degree plies did. The micrograph taken at section C-C shows voids where both matrix and fibers are missing. Evidently, many transthickness and intralaminar cracks had developed in these areas. The sketch on Figure 6 shows that the transthickness cracks extend much further from the notch than in the tension case (Figure 5).

Micrographs of the second stacking sequence $(45/0/-45/0)_s$ laminates taken after 10^7 tension or compression load cycles show damage very similar to that shown on Figures 5 and 6, namely, the development of transthickness and intralaminar cracks. But, in contrast to the $(0/\pm45/0)_s$ case, more intralaminar cracks developed in the 0-degree plies at the edge of the hole for both tension and compression loads.

In summary, micrographs taken after 10^7 tension or compression load cycles showed that intralaminar and transthickness matrix cracks were predominant in the $(0,\pm45)$ laminates. These micrographs showed that intralaminar cracks, primarily in the 45-degree plies, developed around the edge of the hole and that transthickness cracks and intralaminar cracks in the ±45-degree plies developed in narrow bands that were parallel to the loading axis and tangent to the hole. Furthermore, they showed that these matrix cracks were more extensive under compression loads.

Micrographs taken after 10^6 tension or compression load cycles showed only intralaminar cracks around the edge of the hole. Thus, the intralaminar cracks probably occurred before the transthickness cracks.

Fatigue Damage Sequence

From corresponding radiographs and micrographs (those taken of a specimen at identical numbers of load cycles) several observations were made. First, intralaminar cracks around the hole frequently occurred without any fiber breaks. Second, transthickness and local intralaminar cracks in the ±45-degree plies occasionally occurred without any fiber breaks. Third, fibers broke primarily in areas where transthickness and local intralaminar cracks occurred. In these areas fibers frequently broke outside of the area where the transthickness cracks occurred, but

always within the area where local intralaminar cracks in the ±45-degree plies occurred.

On the basis of the previous discussion and the discussions on fiber and matrix damage, the following sequence of events for fatigue of (0,±45) laminates is postulaced:

1. Intralaminar cracks developed around the edge of the hole.

2. Transthickness and local intralaminar cracks in the ±45-degree plies developed in narrow bands parallel to the loading axis and tangent to the hole.

3. In these bands the ±45-degree fibers that were loaded in maximum tension broke.

4. In the same area, the other 45-degree fibers that were loaded in compression broke.

(0,±45,90) Laminates

Fiber Damage

Fibers broke in the (0,±45,90) laminates only under tension loads. As a typical example, Figure 7 shows where fibers broke in the right half-plane of the $(45/0/-45/0)_s$ laminate (similar breaks occurred in the left half-plane). On the figure, open symbols represent breaks in either ±45-degree fibers while the shaded symbols represent breaks in the 0-degree fibers; no 90-degree fibers broke. The different shaped symbols indicate the number of cycles at which the fiber breaks were detected.

In contrast to the (0,±45) laminates, Figure 7 shows that both 0-degree and ±45-degree fibers broke in a band that was perpendicular to the loading axis rather than parallel to it. Near the hole, both 0-degree

and ±45-degree fibers broke, but away from the hole only ±45-degree fibers broke. About 10 percent of both the 0-degree and the ±45-degree fibers across the specimen width broke. Most of the breaks occurred between 6×10^6 and 10^7 load cycles.

Matrix Damage

Matrix damage in the $(0,\pm45,90)$ laminates occurred primarily as intralaminar matrix cracks; no transthickness matrix cracks were apparent. As a typical example, Figure 8 shows matrix damage in a $(90/\pm45/0)_s$ laminate after 10^7 tensile load cycles. The micrographs taken at sections A-A and B-B show intralaminar cracks have developed along the transverse centerline of the specimen. In contrast, the $(0,\pm45)$ laminates did not develop intralaminar cracks in this area. The micrograph taken at view C-C shows typical intralaminar damage around the edge of the hole.

Figure 9 shows two micrographs of matrix damage in a $(90/\pm45/0)_s$ laminate after 10^7 compression load cycles. Unlike a similar laminate cycled under tension, this laminate exhibited intralaminar cracks primarily in the 0-degree plies rather than in the 45-degree plies.

Micrographs taken of $(45/90/-45/0)_s$ laminates tested under either tensile or compressive loads showed damage similar to that which occurred in the $(90/+45/0)_s$ laminates. But under compressive loads intralaminar cracks occurred in the ±45-degree plies along the transverse centerline of the specimen.

In summary, the matrix damage in the $(0,\pm45,90)$ laminates after 10^7 load cycles occurred as intralaminar cracks around the edge of the hole and along the transverse centerline of the specimen. Around the hole,

both the stacking sequence and the sign of the applied load (tension or compression) determined which plies cracked. Along the transverse centerline intralaminar cracks generally developed in ±45-degree plies. Micrographs taken at different numbers of load cycles suggest that the intralaminar cracks in the ±45-degree plies progress across the width of the specimen as more load cycles are applied.

Fatigue Damage Sequence

From corresponding radiographs and micrographs several observations were made. First, intralaminar cracks around the hole develop. Second, intralaminar cracks along the transverse centerline of the specimen occasionally developed without any fiber breaks. Third, fiber breaks only occurred after intralaminar cracks in the ±45-degree plies occurred earlier.

Based on preceding discussions, the following sequence of events for fatigue of (0,±45,90) laminates is postulated:

1. Intralaminar cracks developed around the edge of the hole.

2. Intralaminar cracks in ±45-degree plies extended from the edge of the hole along the transverse centerline of the specimen.

3. Near the hole, 0-degree and the ±45-degree fibers broke where intralaminar cracks in the ±45-degree plies had occurred.

4. Further away from the hole ±45-degree fibers broke where intralaminar cracks in the ±45-degree plies had occurred.

5. Catastrophic failure followed.

Summary of Microsopic Damage

Initially, fatigue damage in both (0,±45) and (0,±45,90) laminates occurred as intralaminar cracks around the edge of the hole. Then, whenever further damage developed, intralaminar cracks in the ±45-degree plies began to propagate from the edge of the hole. For the (0,±45) laminates these cracks occurred simultaneously with transthickness cracks and propagated along lines parallel to the loading axis, whereas for the (0,±45,90) laminates no transthickness cracks occurred and damage propagated along lines perpendicular to the loading axis. Finally, in both type laminates fibers broke where intralaminar cracks in the ±45-degree plies had occurred. In both type laminates primarily ±45-degree fibers broke (prior to final failure).

Macroscopic Behavior

Figure 10 shows the effect of tensile cyclic loads on the effective modulus of the four different notched laminates tested. The effective modulus is calculated as

$$E^* = \frac{\sigma_{max} L}{\delta} \quad (1)$$

where δ is the measured deflection over a gage length, L, of 10 cm, and σ_{max} is the maximum applied gross stress of 318 MPa and 191 MPa for the (0,±45) and (0,±45,90) laminate types respectively.

Typically, for both notched and unnotched (0,±45) laminates about a three percent change in effective modulus occurred. However, in a few

tests wherein the longitudinal damage (transthickness and intralaminar matrix cracks and ±45-degree fiber breaks) was extensive, the modulus decreased about ten percent. The additional decrease in modulus most likely resulted when the longitudinal damage rendered a significant portion of the material above and below the hole ineffective. If the longitudinal damage extended to the grips, the decease in modulus would at least sixteen percent.

For both notched and unnotched (0,±45,90) laminates, the modulus decreased about fiftenn percent. Because the modulus decreased the same for both the notched and unnotched laminates, the damage due to the stress concentrations around the hole must have been too localized to affect the modulus. Also, figure 10 shows that the modulus decreased before a million cycles, but figure 7 shows that most fibers broke after a million cycles. Apparently, the decrease in modulus is predominatly a function of matrix degradation.

Figure 11 shows the net failure stress of virgin laminates as diamonds, the residual strength after 10^7 cycles as squares, and fatigue failures occurring before 10^7 tensile load cycles as triangles labeled with the number of cycles to failure. For reference, a few unnotched specimens were also tested; these tests results are shown by shaded symbols.

As is evident from the figure, the (0,±45) laminates retained strength for the duration of the fatigue test. Evidently, the transthickness and intralaminar matrix cracks and ±45-degree fiber breaks which occurred parallel

to the loading axis had little effect on axial strength. In contrast, the (0,±45,90) laminates, where intralaminar matrix cracks and ±45-degree fiber breaks occurred along the transverse centerline, lost strength as they were fatigued and frequently failed catastrophically.

As previously discussed, microscopic damage, intralaminar cracks and fiber breaks in both type laminates occurred primarily in the ±45-degree plies. Apparently, the residual strength behavior in the two types of laminates depended upon whether the damage propagated parallel or transverse to the loading axis.

CONCLUDING REMARKS

Two families of laminates, (0,±45) and (0,±45,90) with two different stacking sequences were fatigue tested under constant amplitude tension or compression loads. In these laminates fatigue damage in the fibers and matrix were studied with X-ray radiography and scanning electron microscopy. In addition limited tests for residual strength and stiffness were performed.

Initially, fatigue damage in both (0,±45) and (0,±45,90) laminates occurred as intralaminar cracks in the matrix around the edge of the hole. Whenever further damage developed, intralaminar cracks in the ±45-degree plies began to propagate from the edge of the hole. Finally, in both type laminates primarily ±45-degree fibers broke where intralaminar cracks in the ±45-degree plies had occurred. In the (0,±45) laminates, the 45-degree plies developed intralaminar matrix cracks in bands parallel to the loading axis and tangent to the hole in the test specimen. Damage in the (0,±45) laminates was

most pronounced under compression loads and had little effect on either residual strength or stiffness. In contrast, in the (0,±45,90) laminates, the ±45-degree plies developed intralaminar matrix cracks in a band transverse to the loading axis. The damage in these laminates occurred primarily under tension loads, reduced the residual strength and frequently resulted in catastrophic failure across the notch. All results of this study suggest that the 45-degree plies play a key role in the fatigue process of boron/epoxy laminates that contain them.

REFERENCES

1. Durchlaub, E. C., and Freeman, R. B., "Design Data for Composite Structure Safelife Prediction," AFML-TR-73-225 (Volume 1), March 1974.

2. Foye, R. L., and Baker, D. J., "Design of Orthotropic Laminates," AIAA/ASME 11th Conf. Structures, Structural Dynamics, and Materials, Denver, Colorado, April 1970.

3. Williams, R. S., and Reifsnider, K. L., "Fracture Analysis of Fatigue Damage Mechanisms in Fiber Reinforced Composite Materials Using Scanning Electron Microscopy," AFOSR-TR-75-0041, 1975.

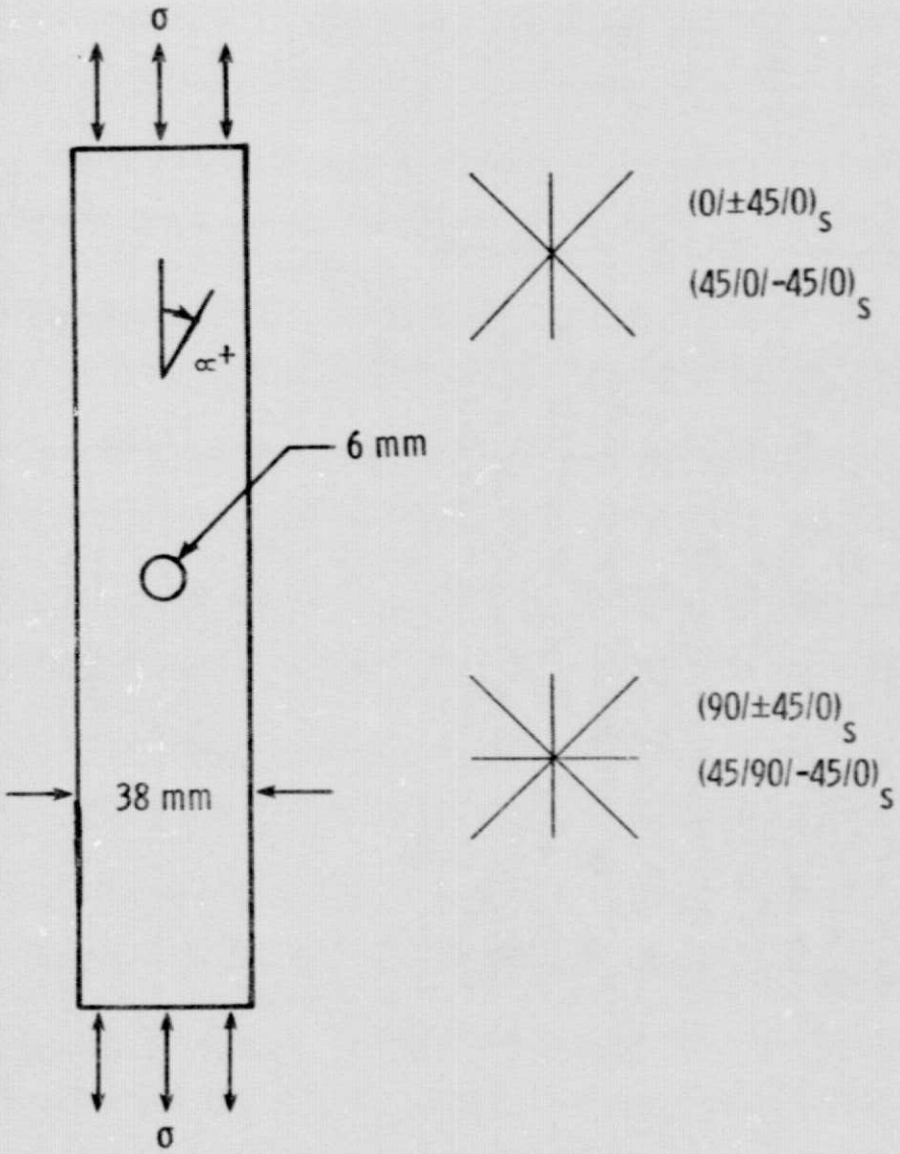

Figure 1. Specimen configuration and loading

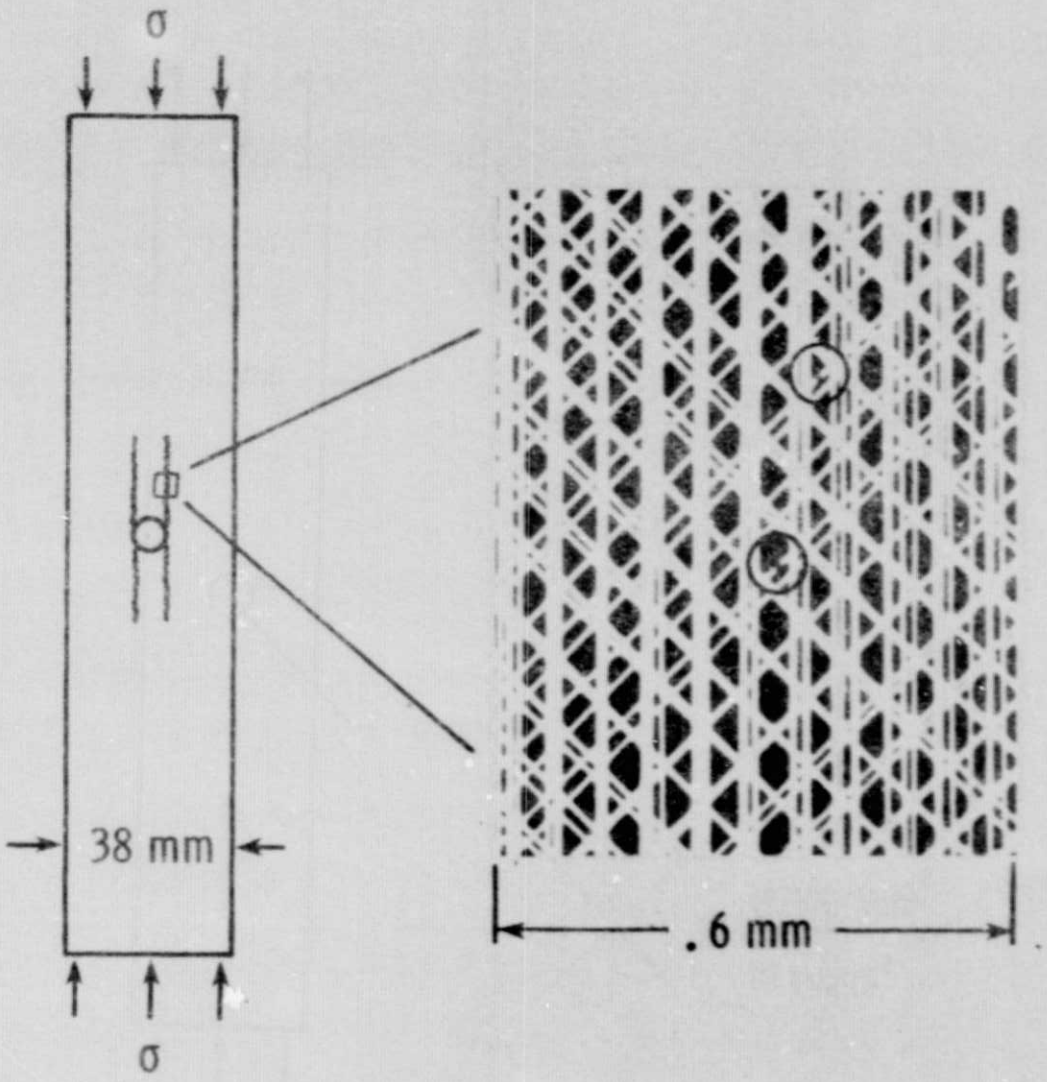

Figure 2. Radiograph of typical fiber breaks

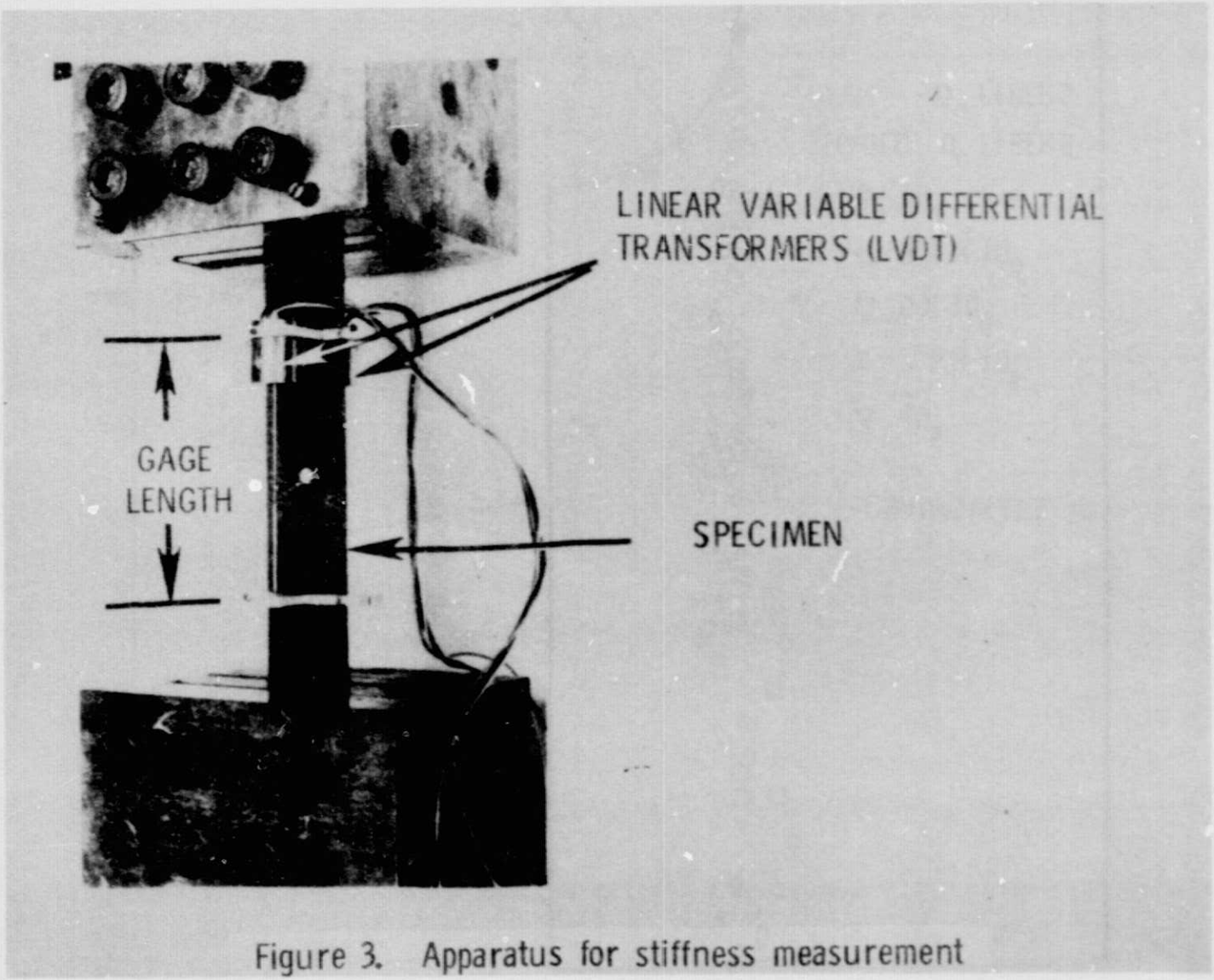

Figure 3. Apparatus for stiffness measurement

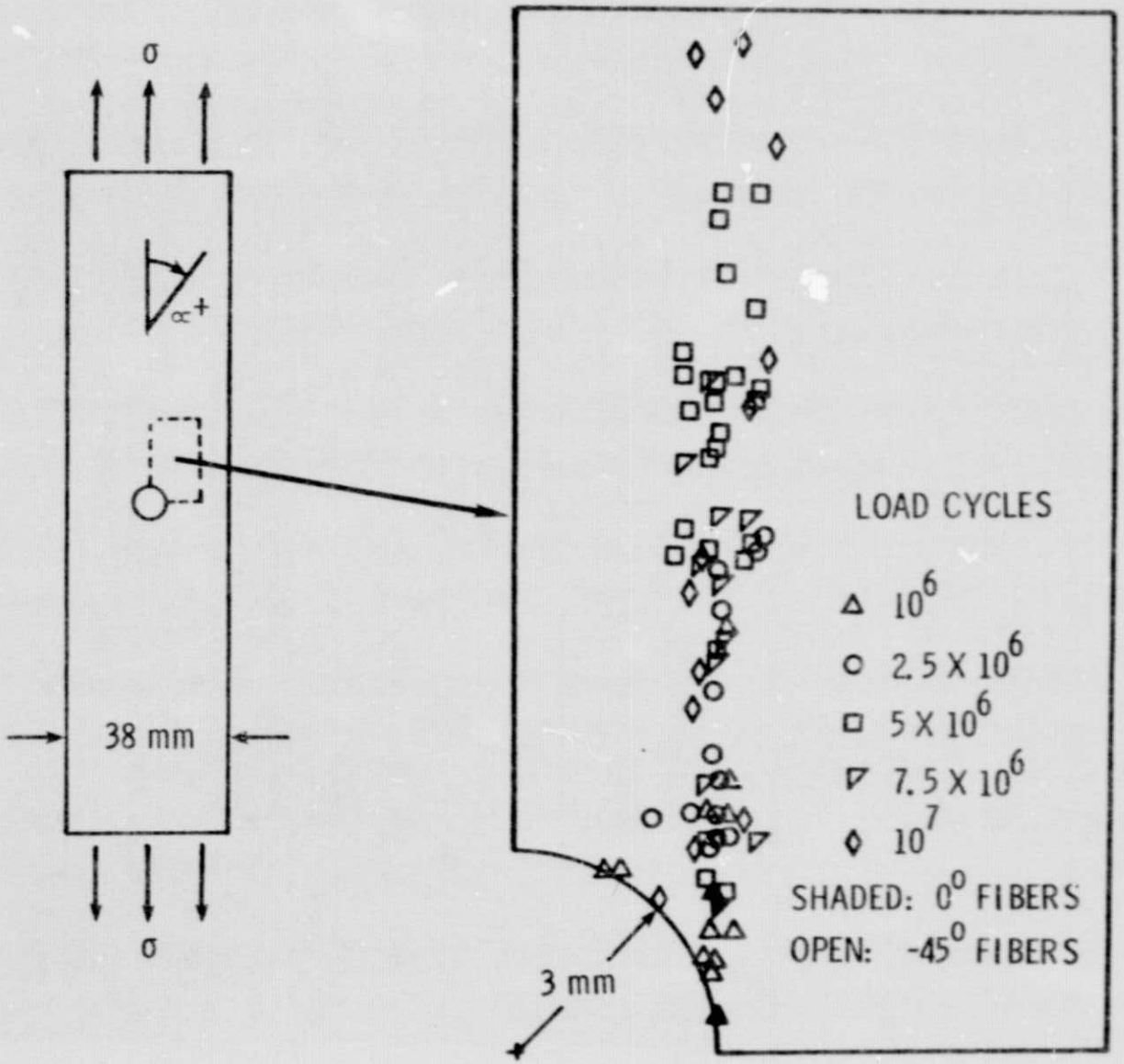

Figure 4. Fiber failures in a $(45/0/-45/0)_s$ laminate under cyclic loading

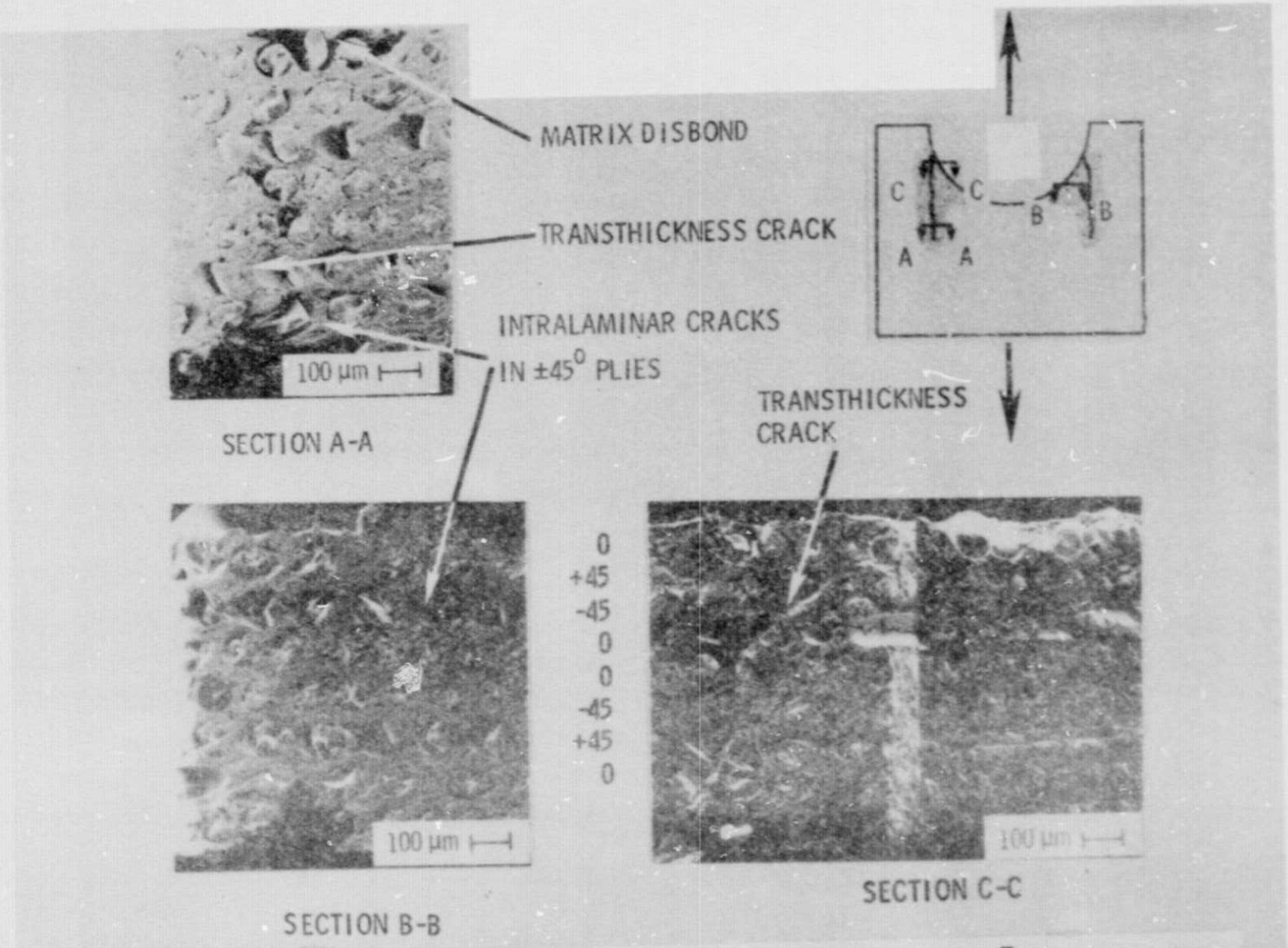

Figure 5. Matrix damage in a $(0/\pm45/0)_S$ laminate after 10^7 tension loads

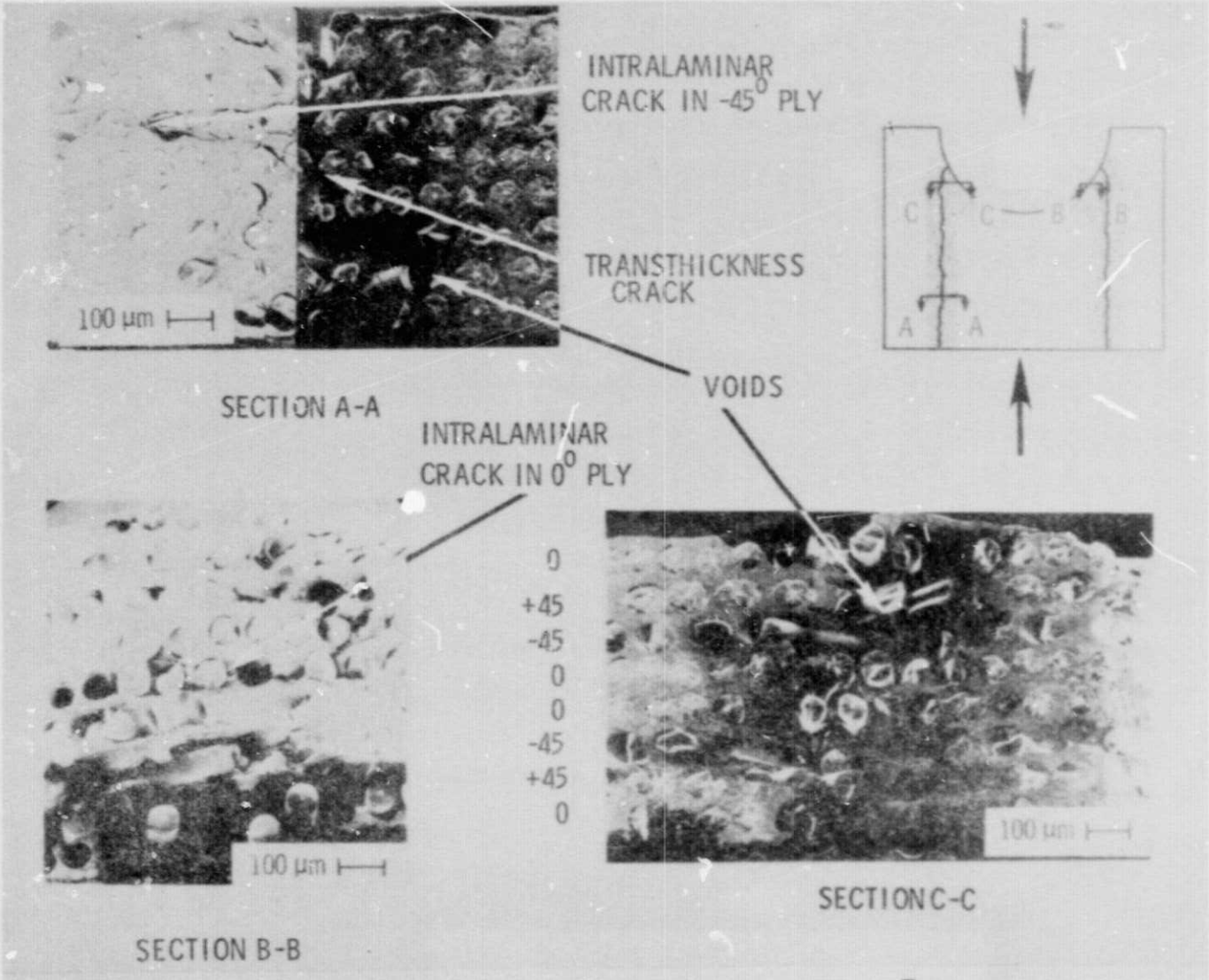

Figure 6. Matrix damage in a $(0/\pm45/0)_s$ laminate after 10^7 compression loads

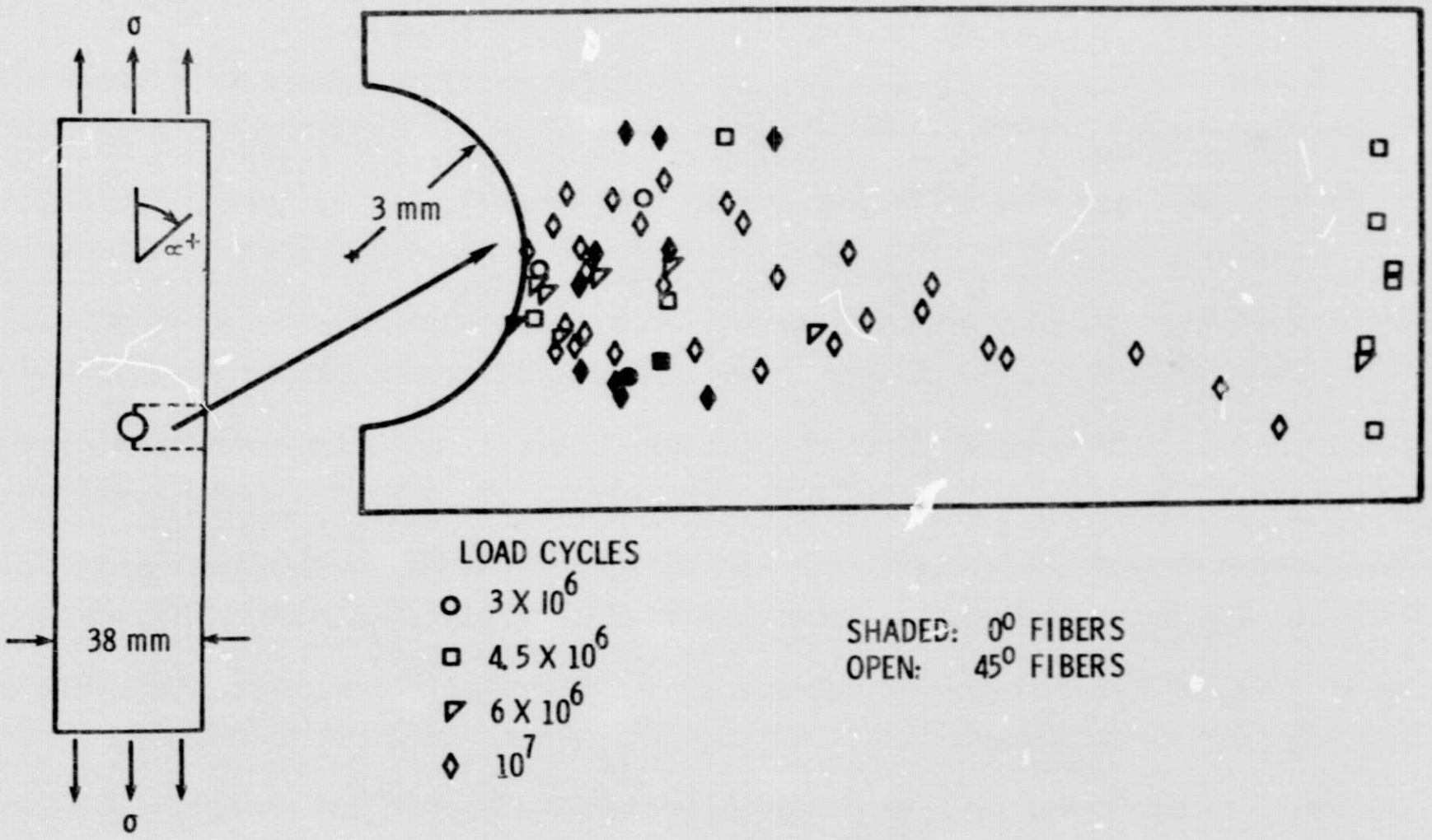

Figure 7. Fiber failures in a $(45/90/-45/0)_S$ laminate under cyclic loads

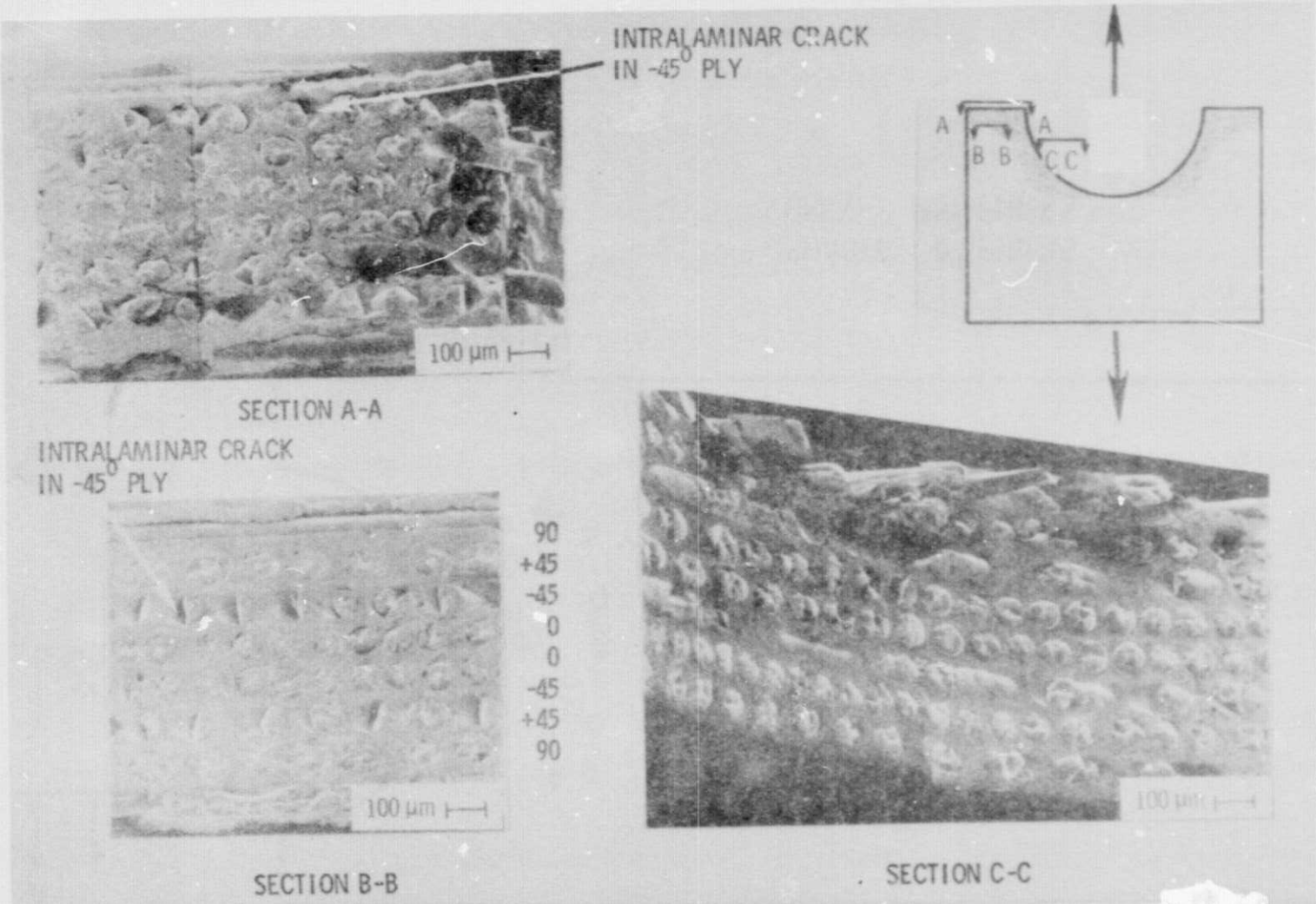

Figure 8. Matrix damage in a $(90/\pm45/0)_S$ laminate after 10^7 tension loads

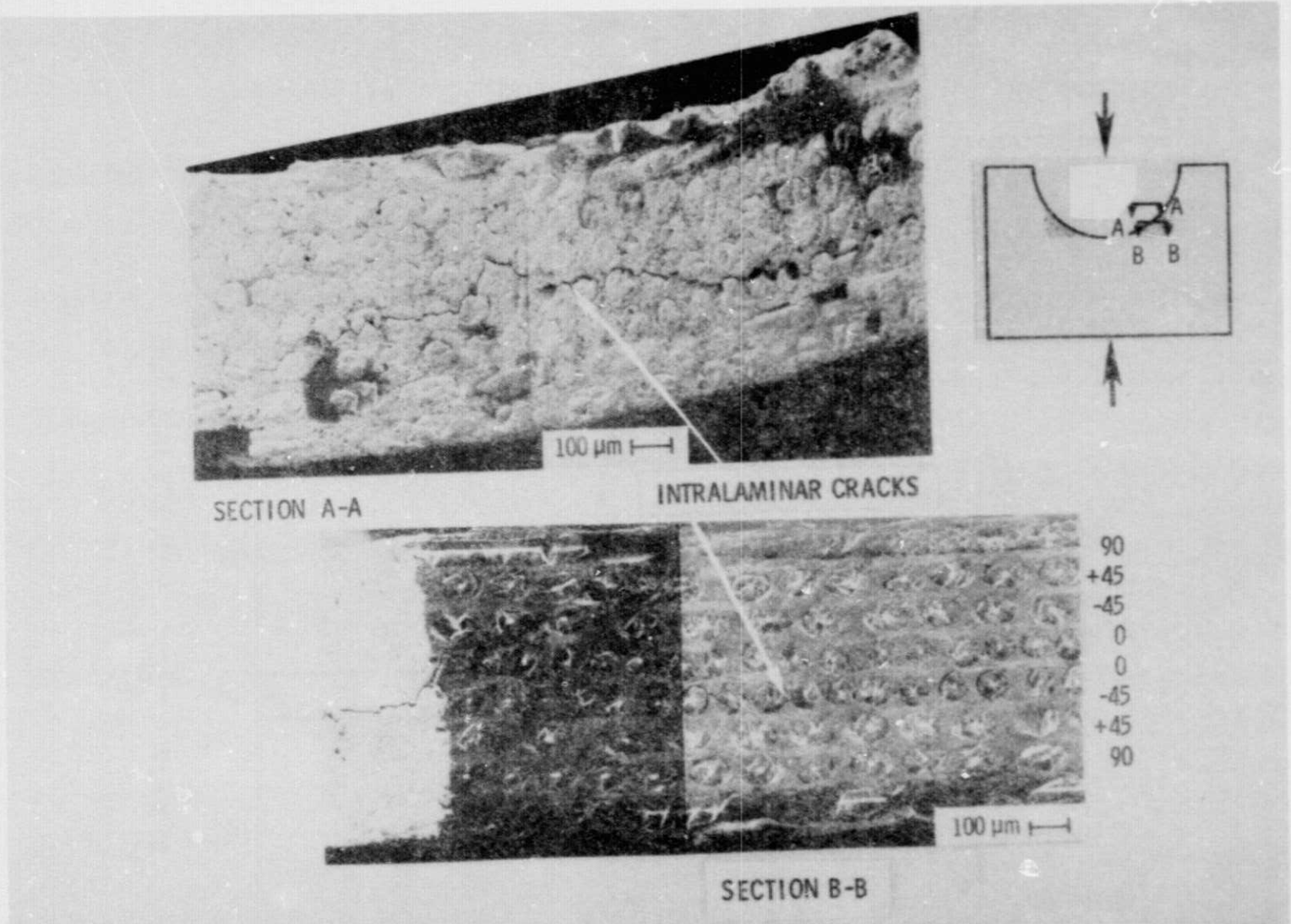

Figure 9. Matrix damage in a $(90/\pm45/0)_S$ laminate after 10^7 compression loads

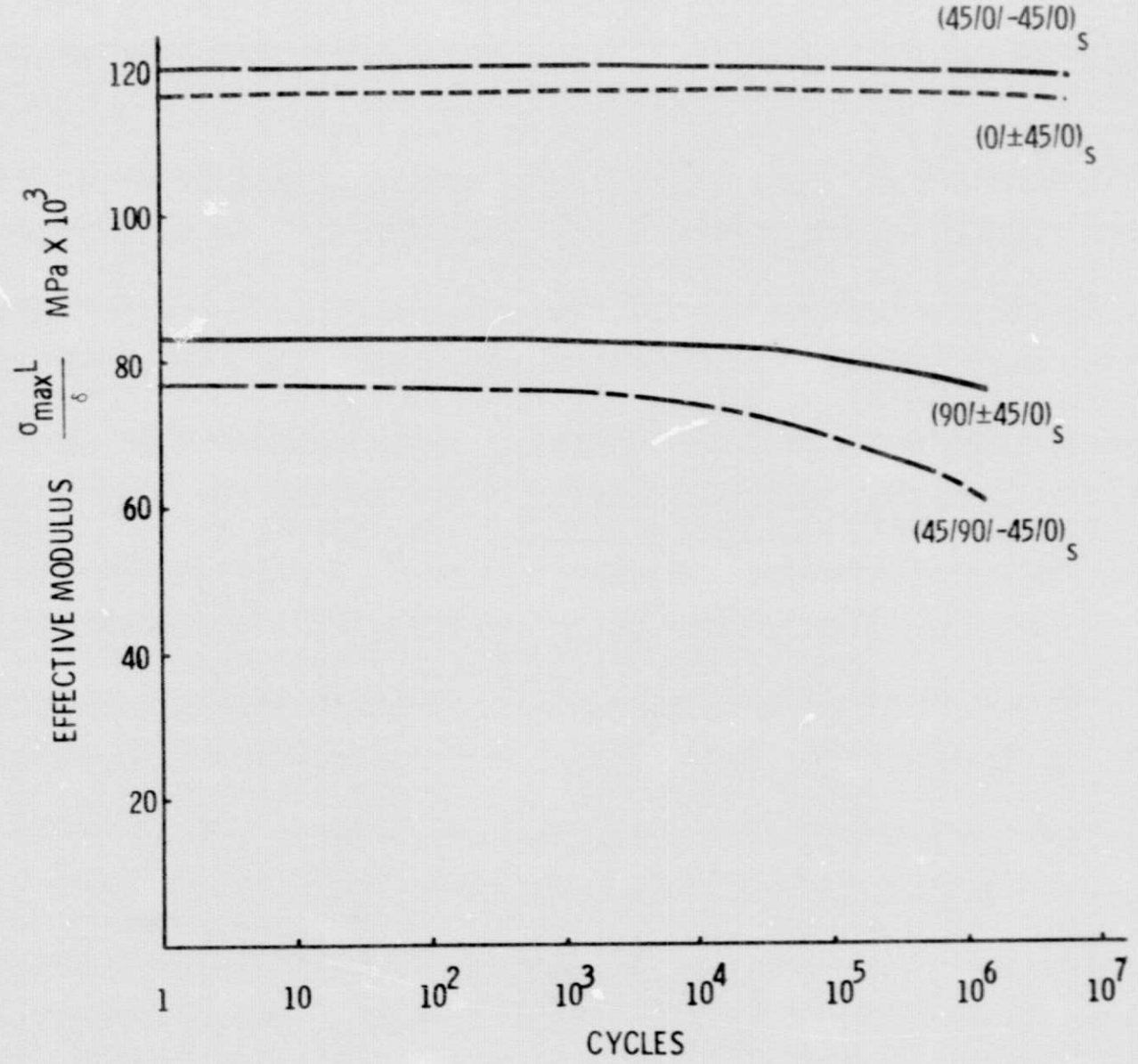

Figure 10. Modulus change during tension fatigue

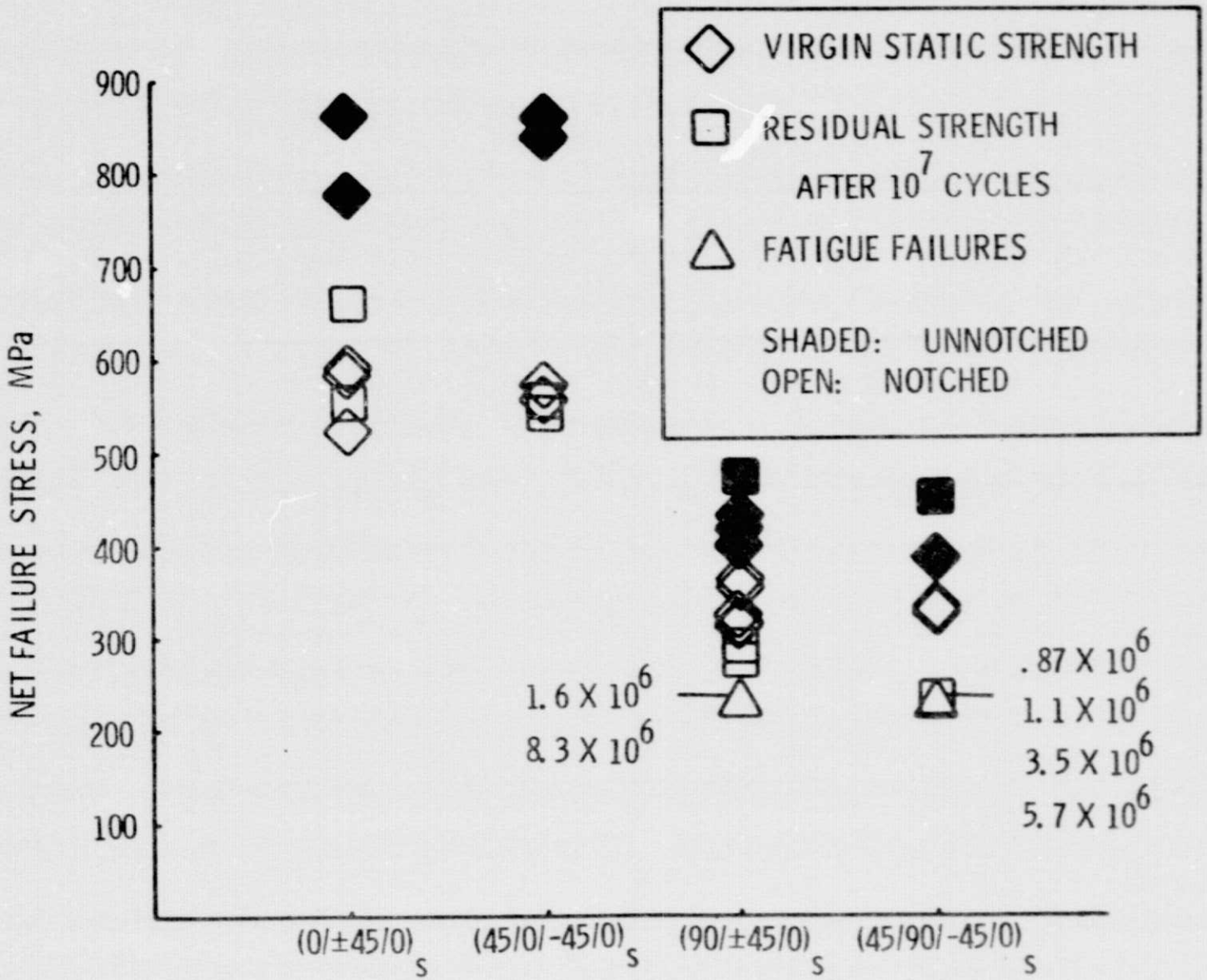

Figure 11. Residual strength after tension fatigue